Anal. Chem. **2006,** *78,* 2526−2531

Label-Free Microelectronic PCR Quantification

Chih-Sheng Johnson Hou,[†] Nebojsa Milovic,[‡] Michel Godin,[‡] Peter R. Russo,[†] Raj Chakrabarti,[‡,§,⊥] and Scott R. Manalis*[,‡,∥]

Department of Electrical Engineering and Computer Science, Biological Engineering Division, Department of Chemistry, and Department of Mechanical Engineering, Massachusetts Institute of Technology, Cambridge, Massachusetts 02139, and Department of Chemistry, Columbia University, New York, New York 10025

We present a robust and simple method for direct, label-free PCR product quantification using an integrated microelectronic sensor. The field-effect sensor can sequentially detect the intrinsic charge of multiple unprocessed PCR products and does not require sample processing or additional reagents in the PCR mixture. The sensor measures nucleic acid concentration in the PCR relevant range and specifically detects the PCR products over reagents such as Taq polymerase and nucleotide monomers. The sensor can monitor the product concentration at various stages of PCR and can generate a readout that resembles that of a real-time fluorescent measurement using an intercalating dye but without its potential inhibition artifacts. The device is mass-produced using standard semiconductor processes, can be reused for months, and integrates all sensing components directly on-chip. As such, our approach establishes a foundation for the direct integration of PCR-based in vitro biotechnologies with microelectronics.

The introduction of real-time monitoring of the polymerase chain reaction (PCR) represents a major breakthrough in specific nucleic acid quantification. This technique employs fluorescent intercalating agents[1] or sequence-specific reporter probes[2,3] to measure the concentration of amplified products after each PCR cycle. It enables a wide range of nucleic acid measurements of up to 8 orders of magnitude, high sensitivity of fewer than 5 copies, and high precision of less than 2% standard deviation.[4] However, the need for optical components can limit the scalability and robustness of the measurement for miniaturization and field uses, and the addition of external fluorescent reagents can induce inhibitory effects[5,6] and require extensive optimization.[7]

Various nonoptical label-free sensing methods have been developed to quantify biomolecules on the basis of their intrinsic properties.[8−17] Typically, these sensing techniques quantify nucleic acids by hybridization of free single-stranded targets in solution to immobilized single-stranded complementary probes. Since PCR generates double-stranded DNA (dsDNA), extra steps are necessary to generate single-stranded DNA (ssDNA) or RNA for hybridization. For example, sample preparation can require heating followed by rapid cooling of the product to prevent renaturation[18] or in vitro transcription of double-stranded products to generate single-stranded RNA.[19] These additional steps increase the complexity of tasks that require repetitive assays, such as real-time quantitative PCR. Furthermore, surface recovery for repeated analysis using the same DNA capturing probe layer may reduce sensitivity due to damage sustained after repeated rinsing to dissociate bound products.[14]

Here, we demonstrate quantitative label-free monitoring of product formation in an unprocessed PCR mixture using a microelectronic sensor based on silicon field effect. We achieve high sensitivity to the intrinsically charged PCR product by depositing a thin layer of poly-L-lysine (PLL) on the charge-sensitive region of the sensor. In this configuration, the sensor can quantitatively and reproducibly differentiate concentrations of DNA in the PCR relevant range of 1−80 ng/μL. After measuring a particular concentration, the sensor can be readily recovered by depositing another layer of PLL on the sensor surface without degrading the sensitivity. Thus, the technique is capable of

* To whom correspondence should be addressed. Phone: (617) 253 5039. Fax: (617) 253 5102. E-mail: scottm@media.mit.edu.
† Department of Electrical Engineering and Computer Science, MIT.
‡ Biological Engineering Division, MIT.
§ Department of Chemistry, MIT.
∥ Department of Mechanical Engineering, MIT.
⊥ Columbia University.

(1) Higuchi, R.; Fockler, C.; Dollinger, G.; Watson, R. *Biotechnology* **1993**, *11*, 1026−1030.
(2) Tyagi, S.; Kramer, F. R. *Nat. Biotechnol.* **1996**, *14*, 303−308.
(3) Heid, C. A.; Stevens, J.; Livak, K. J.; Williams, P. M. *Genome Res.* **1996**, *6*, 986−994.
(4) Klein, D. *TRENDS Mol. Med.* **2002**, *8*, 257−260.
(5) Nath, K.; Sarosy, J. W.; Hahn, J.; Di Como, C. J. *J. Biochem. Biophys. Methods* **2000**, *42*, 15−29.
(6) Monis, P. T.; Giglio, S.; Saint, C. P. *Anal. Biochem.* **2005**, *340*, 24−34.
(7) Boeckh, M.; Huang, M.; Ferrenberg, J.; Stevens-Ayers, T.; Stensland, L.; Nichols, W. G.; Corey, L. *J. Clin. Microbiol.* **2004**, *42*, 1142−1148.
(8) Fritz, J.; Cooper, E. B.; Gaudet, S.; Sorger, P. K.; Manalis, S. R. *Proc. Natl. Acad. Sci. U.S.A.* **2002**, *99*, 14142−14146.
(9) Hahm, J.; Lieber, C. M. *Nano Lett.* **2004**, *4*, 51−54.
(10) Fritz, J.; Baller, M. K.; Lang, H. P.; Rothuizen, H.; Vettiger, P.; Meyer, E.; Güntherodt, H.-J.; Gerber, C.; Gimzewski, J. K. *Science* **2000**, *288*, 316−318.
(11) Woods, S. J. *Microchem. J.* **1993**, *47*, 330−337.
(12) Nelson, B. P.; Grimsurd, T. E.; Liles, M. R.; Goodman, R. M.; Corn, R. M. *Anal. Chem.* **2001**, *73*, 1−7.
(13) Macanovic, A.; Marquette, C.; Polychronakos, C.; Lawrence, M. F. *Nucleic Acids Res.* **2004**, *32*, e20−e20(1).
(14) Fan, C.; Plaxco, K. W.; Heeger, A. J. *Proc. Natl. Acad. Sci. U.S.A.* **2003**, *100*, 9134−9137.
(15) Armistead, P. M.; Thorp, H. H. *Anal. Chem.* **2000**, *76*, 3764−3770.
(16) Zheng, G.; Patolsky, F.; Cui, Y.; Wang, W. U.; Lieber C. M. *Nat. Biotechnol.* **2005**, *23*, 1294−1301.
(17) Schöning, M. *Sensors* **2005**, 5, 126−138.
(18) Lucarelli, F.; Marrazza, G.; Mascini, M. **2005**, *20*, 2001−2009.
(19) Innis, M. A.; Gelfand, D. H.; Sninsky, J. J.; White, T. J. *PCR Protocols: A Guide to Methods and Applications*; Academic Press: San Diego; 1990.

10.1021/ac0520689 CCC: $33.50
Published on Web 03/02/2006

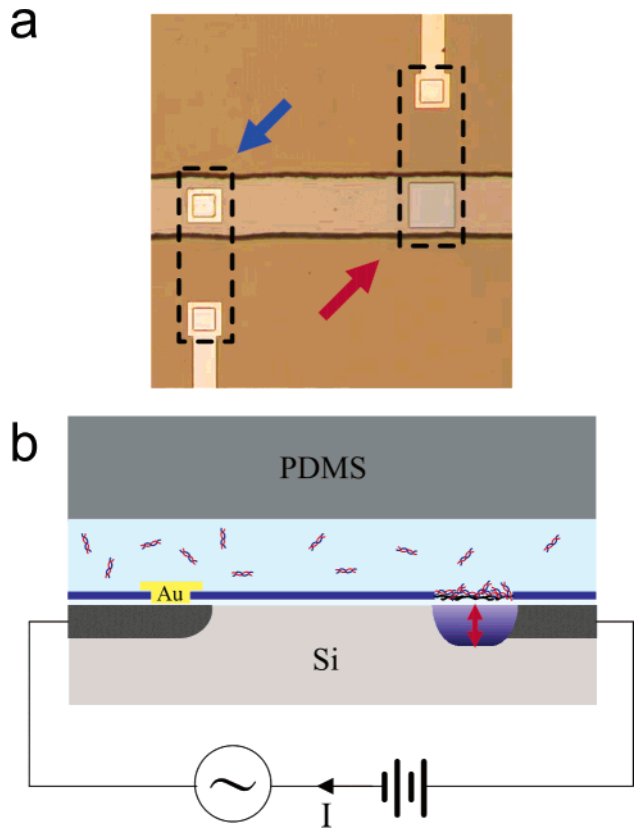

Figure 1. Sensor illustrations. (a) Optical micrograph showing a gold signal electrode (blue arrow, left) and a p-type field-effect sensor (red arrow, right) separated by 400 μm and encapsulated by a horizontal PDMS microfluidic channel. Highly doped buried conductive traces (dotted lines) connect the signal electrode and the field-effect sensor to their respective gold traces away from the channels. (b) Conceptual cross-sectional drawing demonstrating the basis of the device measurement. Binding of charged molecules, such as DNA on the sensor's surface, alters the distribution of positive mobile charge carriers in silicon and results in a modulation of the depletion depth (red arrow), hence changing the capacitance. This change in capacitance is monitored by applying an AC voltage to the gold electrode through the buried conductive trace in silicon (dark gray) and measuring the resulting current that travels through the solution and across the DC voltage-biased variable capacitor (purple), which is modulated by the surface potential. Parasitic conductance through the bulk silicon is minimized by fixing the potential of an implanted ground plane (not shown). The nonsensor areas are electrically insulated by a layer of silicon nitride (blue) and silicon dioxide (white).

sequentially analyzing PCR products at various stages of the reaction through layer-by-layer assembly in microfluidic channels with nanoliter volumes.

EXPERIMENTAL SECTION

Field-Effect Sensors. The field-effect sensors used in this work (Figure 1a) are oxide-based electrolyte−insulator−semiconductor (EIS) capacitors fabricated on planar silicon substrates and encapsulated by poly(dimethylsiloxane) (PDMS) microfluidic channels. Processing began with 6″ *n*-type (phosphorus doped) 20−50 Ω-cm silicon substrates. Conventional photolithography was used to define implants of active sensor areas (lightly doped p-type), conductive traces (heavily doped p-type), and an isolating ground plane (heavily doped n-type). After annealing, a relatively uniform doping level of 10^{15} atoms/cm^3 down to a depth of 0.8 μm was formed in the sensing regions. An 0.8-μm insulating layer ofsilicon-rich nitride was then deposited. Metal contact holes and 80 × 80 μm^2 sensor areas were then etched in the silicon nitride in a single step. Finally, 30-nm Ti and 1-μm Au were evaporated onto the substrate as conductive traces and patterned using a liftoff process. PDMS microfluidic channels were molded from an SU-8 master, and inlets were punched with a 19-gauge needle. With the exception of ion implantation and PDMS molding, all fabrication steps were performed at Massachusetts Institute of Technology's Microsystems Technology Laboratories.

Surface Potential Measurements. The measurement method has been previously reported in detail.[8] Briefly, a 4-kHz, 50-mV$_{pp}$ ac voltage is delivered to the on-chip gold signal electrode (Figure 1b). The resulting alternating current through the sensor is amplified and converted by a lock-in amplifier to a dc voltage that is proportional to the capacitance of a depletion region in the silicon. The capacitance of the depletion region is a function of the potential difference between the electrolyte−insulator interface and p-type sensor region in the EIS structure. Before an experiment, the bias potential applied to the sensor was set at a level where the slope and linearity of the output versus sensor bias voltage curve are maximized.[22] The relative surface potential response of the sensor as a function of the lock-in amplifier output was calibrated by applying a bias step to the sensor. All surface potential values reported in this paper are relative. Constant fluid flow of 10 μL/min was used for all measurements. Analytes were injected by an autosampler (Hitachi High Technologies America), and signals were recorded at 10 Hz.

Polymerase Chain Reaction. Forward primer, 5′ ATC AAG CAG CCA TGC AAA TG 3′, and reverse primer, 5′ CCT TTG GTC CTT GTC TTA TGT C 3′, were used to amplify a 291-base-pair (bp) fragment of the HIV-1 GAG gene.[20] The PCR buffer consisted of 10 mM Tris−HCl (pH 8.3), 20 mM KCl, and 2 mM $MgCl_2$. The reaction mixture included the PCR buffer, 0.1 mM each of dNTPs, 0.4 μM each of forward and reverse primers, 5 U Taq polymerase (New England BioLabs, Ipswich, MA), and positive control templates (1 ng/mL) (Maxim Biotech, South San Francisco). For real-time PCR, Sybr Green I (Molecular Probes, Eugene, OR) was added to the PCR mixture using a 10 000-fold dilution of the stock solution. The PCR was performed for 35 cycles of 90 °C for 25 s, 53 °C for 30 s, and 72 °C for 50 s or stopping at earlier cycles when necessary. For control experiments, a QIAquick PCR Purification Kit (Qiagen, Valencia, CA) was used to isolate the PCR products from saturated PCR reactions.

Sensor Surface Preparation. The silicon device was submerged in hot piranha solution (1:3 30% H_2O_2 in H_2SO_4) for 5 min. The silicon chip was then rinsed with deionized water, dried with nitrogen, aligned, and hermetically bonded to PDMS. Hydrofluoric acid (buffered oxide etch 7:1) (7:1 H_2O/HF) was introduced into the microfluidic channel for 20 s. PCR buffer was flowed through the channel overnight to equilibrate the sensor. The surface preparation procedure left a thin native oxide on the sensor

(20) http://www.ncbi.nlm.nih.gov/entrez/query.fcgi?cmd=Retrieve&db=Nucleotide&list_uids=328658&dopt=GenBank; accessed on Nov 21, 2005.
(21) Whitesides, G.; Xia, Y. Soft lithography. *Angew. Chem., Int. Ed.* **1998**, *37*, 550−575.
(22) Cooper, E. B.; Fritz, J.; Wiegand, G.; Wagner, P.; Manalis, S. R. *Appl. Phys. Lett.* **2001**, *79*, 3875−3877.

surface. Functionalization of the surface was performed by exposing the sensor surface to 0.2 mg/mL poly-L-lysine hydrobromide (MW 15 000−30 000, Sigma, St. Louis, MO) in PCR buffer for 3 min, then rinsing off the unbound species with PCR buffer for 10−15 min. A DNA dose−response curve was generated by diluting stock 50-bp DNA ladder (New England BioLabs, Ipswich, MA) to various concentrations with PCR buffer. Human genomic DNA used in this study was purchased from Maxim Biotech, Inc (South San Francisco, CA). For all binding experiments on PLL-coated surfaces, the sensors were exposed to analytes for 5 min, followed by a 5-min wash, during which time the signal was recorded. To remove all organics from the sensor surface, PDMS was peeled off the silicon device, and the sensor chip was subsequently cleaned with piranha solution as outlined above.

Real-Time and End-Point PCR Product Quantification. Optical readout of double-stranded DNA synthesis during PCR was carried out in a real-time thermocycler (DNA Engine Opticon System; MJ Research, Watertown, MA) using Sybr Green I Dye. Data were recorded after the primer extension steps (72 °C). Alternatively, quantitative readouts of PCR product concentrations were obtained using DNA 12000 Labchip kits (Agilent, Palo Alto, CA) from PCR reaction completing 15, 20, 25, 30, and 35 cycles without the presence of intercalating dyes. PCR products were frozen immediately after thermocycling and thawed before Labchip gel analysis.

RESULTS AND DISCUSSION

The electronic device, which is encapsulated by poly(dimethylsiloxane) (PDMS) microfluidics,[21] behaves as a variable capacitor whose impedance is sensitive to the charge density of surface-bound molecules.[22,23] Electrostatic surface attachment of nucleic acids can be achieved either by applying a potential to the surface[24,25] or by depositing cationic molecules. We used the latter approach to monitor the formation of polyelectrolyte multilayers through alternating depositions of poly-L-lysine, a positively charged polypeptide, and DNA, which carries two negative charges per base pair. The thickness of polyelectrolyte multilayers is known to increase with alternating depositions of oppositely charged species due to electrostatic associations,[26,27] thus yielding rising signals when measuring their mass or thickness.[28,29] Polyelectrolyte multilayer deposition on the intrinsically negatively charged field-effect sensor surface reveals markedly different behavior; the deposition of a positively charged polymer consistently results in a decrease of signal and the subsequent adsorption of a negatively charged species results in an increase.[8] Figure 2 shows the sensor response to two consecutive rounds of alternating PLL and DNA injections within an experiment during which 18 dielectric layers were deposited. The cyclical pattern was observed without noticeable degradation in the amplitude of the equilibrated signal; 13 mV was recorded for both the first and final layer of DNA deposition, indicating that the overcompensated surface charge at the top layer is effectively propagated to the sensor surface. In addition, even though our technique measures the overall series impedance of the electrical pathway, including that of the multilayer film, that the sensor is primarily sensitive to changes in surface potential rather than to the dielectric properties of the surface. Otherwise, the signal amplitude would decay noticeably with increasing multilayer thickness. At the same time, the additive surface regeneration process ensures that the surface is saturated by positive charges and the binding capacity does not degrade for multiple DNA analyses. After multilayer deposition, cleaning with piranha solution can restore the sensor to its initial state without degrading sensitivity.[8] We have repeated this cleaning procedure on a device that was reused for more than a month.

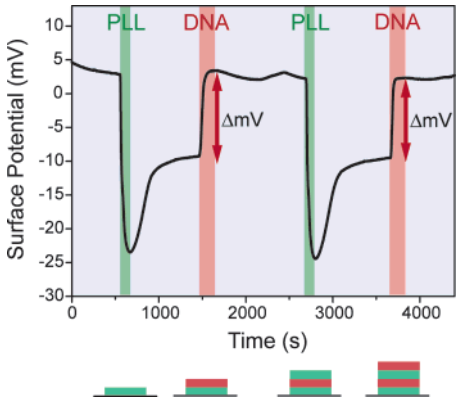

Figure 2. Electronic detection of DNA−poly-L-lysine multilayer depositions. PLL was introduced to the sensor for 3 min (green window), followed by 10 min of rinsing with buffer, after which DNA was introduced for 5 min (red), followed by a 15-min wash. The lower part (not drawn to scale) illustrates conceptually the expected monotonic increase in film thickness for alternating exposures to PLL and DNA solution, in contrast to the cyclical patterns (increase for DNA and decrease for PLL) observed for the electronic measurements.

We tested the sensor's response to DNA concentrations in the range relevant to PCR conditions to determine its utility for PCR analysis. To obtain the DNA mass concentration response of the sensor, we chose a DNA ladder of lengths between 50 and 1350 bp, which is representative of various PCR product sizes (Figure 3a). It was empirically determined using the Labchip kits that product concentrations between 20 and 50 ng/μL are obtained from various saturated PCR experiments (data not shown). Therefore, we tested the dependence of surface potential change on DNA concentration between 2.5 and 80 ng/uL. The dose−response curve (Figure 3b) shows that the device is most sensitive to DNA concentration between 10 and 40 ng/μL, a range relevant to PCR quantifications.

The electronic detection of DNA/PLL multilayers is useful for PCR product analysis if the measurement is only sensitive to the products of interest in a PCR mixture. To characterize this, the PLL-coated surface of the sensor was exposed to the individual components present in a PCR mixture: Taq polymerase; dNTP; and DNA, including primers, templates, and PCR products. The components were introduced at the same concentrations used for PCR to quantify their corresponding surface potential response.

(23) Bousse, L.; Bergveld, P. *J. Electroanal. Chem.* **1983**, *152*, 25−39.
(24) Wang, J.; Zhang X. J.; Parrado C.; Rivas G. *Electrochem. Commun.* **1999**, *1* (6), 197−202.
(25) Kara, P.; Kerman, K.; Ozkan, D.; Meric B.; Erdem A.; Nielsen, P. E.; Ozsoz, M. *Electroanalysis* **2002**, *14*, 1685−1690.
(26) Decher, G. *Science* **1997**, *277*, 1232−1237.
(27) Lvov, Y.; Decher, G.; Sukhorukov, G. *Macromolecules* **1994**, *26*, 5396−5399.
(28) Pei, R.; Cui, X.; Yang, X.; Wang, E. *Biomacromolecules* **2001**, *2*, 463−468.
(29) Wink, T.; de Beer, J.; Hennink, W. E.; Bult, A.; van Bennekom, W. P. *Anal. Chem.* **1999**, *71*, 801−805.

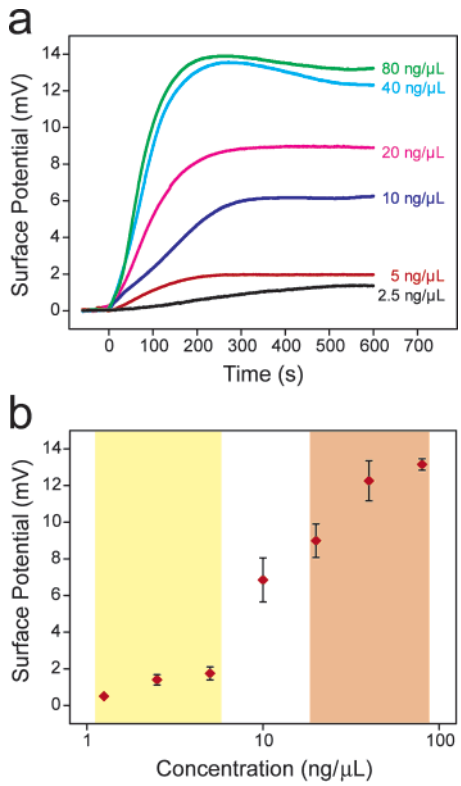

Figure 3. DNA concentration response of the electronic sensor. Sensitivity response to individual components in a PCR reaction. (a) DNA ladder (50−1350 bp) at various dilutions was used to obtain an average-case response for PCR products of 1 kb or shorter. Samples were injected in order of increasing concentrations, that is, from 1.25 to 80 ng/μL. PLL solution was injected between measurements to regenerate the sensor surface. DNA in PCR buffer was introduced to the sensor for 5 min, followed by a 5-min rinse in buffer. (b) Steady-state response following sensor rinsing is shown as a function of DNA concentration. The yellow window indicates the typical total concentration of nucleic acid at the start of the PCR reaction, including the primers and templates; the red window indicates a range of expected product concentrations at PCR saturation. The error bars represents 1 SD above and below the average sensor output for multiple injections of a given concentration. Samples were injected in no particular order.

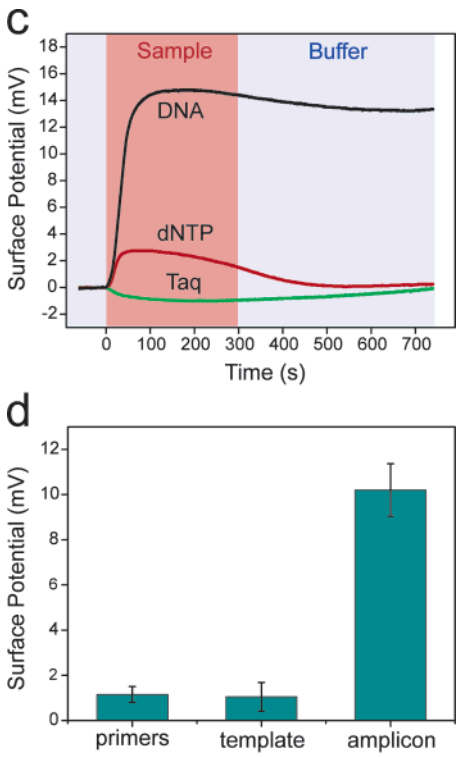

Figure 4. Sensitivity assessment for individual components in a PCR reaction. (a) The sensor's response to PCR components, including DNA (40 ng/μL), dNTP (0.1 mM each), and Taq polymerase (0.05 U/μL), at concentrations relevant to PCR conditions were introduced to the PLL-coated sensors for 5 min and flushed with PCR buffer for 5 min. Upon rinsing, only DNA yielded consistent changes from the baseline signal. (b) The steady-state surface potential responses following the injections of primers (0.4 μM 20-bp forward and 22-bp reverse primers), 2 ng/μL genomic DNA, and 30 ng/μL purified amplification product. Error bars represent 1 SD above and below the average surface potential changes.

Taq polymerase decreased the surface potential slightly during its introduction (Figure 4a), but the baseline potential was recovered after subsequent rinsing. The dNTP solution raised the sensor output during injection, but the change was again not permanent. Although dNTP has four negative charges per molecule, this result shows that permanent electrostatic adsorption requires stronger multivalent interactions between the molecules in solution and the surface to prevent elution by buffer. In contrast, 40 ng/μL of dsDNA ladder resulted in a clearly resolvable baseline shift.

The types of nucleic acids in a PCR mixture include primers, templates, and products. The sensor's response to each component was characterized at the concentrations used for the PCR experiments. In particular, the sensor's response to 0.4 μM forward and reverse primers, 2 ng/μL genomic DNA (equivalent to 100 ng DNA template in 50 μL of PCR buffer), and 30 ng/μL purified amplification product yielded average surface potential changes of 1, 1, and 10 mV, respectively (Figure 4b). This result indicates that even though the primers and templates in a PCR mixture will produce background signals, the product is expected to contribute most significantly to the overall sensor readout when PCR saturates.

On the basis of the data, several inferences can also be made about the sensitivity of the electronic sensor to DNA length. The 0.4 μM, 20-bp forward and 22-bp reverse primers account for a mass concentration of ~5 ng/μL and resulted in an output similar to that of DNA ladder at the same mass concentration. Similarly, 2 ng/μL of genomic DNA, 90% of which was expected to be larger than 50 kbp, according to manufacturer's analysis, produced a signal comparable to that of 2 ng/μL DNA ladder. Finally, 30 ng/μL of purified product yielded a surface potential change of 10 mV, which is between the average surface potential measurements for 20 and 40 ng/μL ladders. These comparisons show that for concentrations relevant to PCR, the measurement method is sensitive primarily to the mass concentration of nucleotides rather than to the length of DNA.

A segment of the HIV-1 GAG gene was amplified, and the products were analyzed at various stages of the reaction. Figure 5a shows the temporal response of the electronic detector, and Figure 5b shows the comparison of endpoint measurements by optical detection with an intercalating dye, by gel electrophoresis, and by electronic detection. Real-time Sybr Green I fluorescence readout showed a marked increase after ~20 cycles of amplifica-

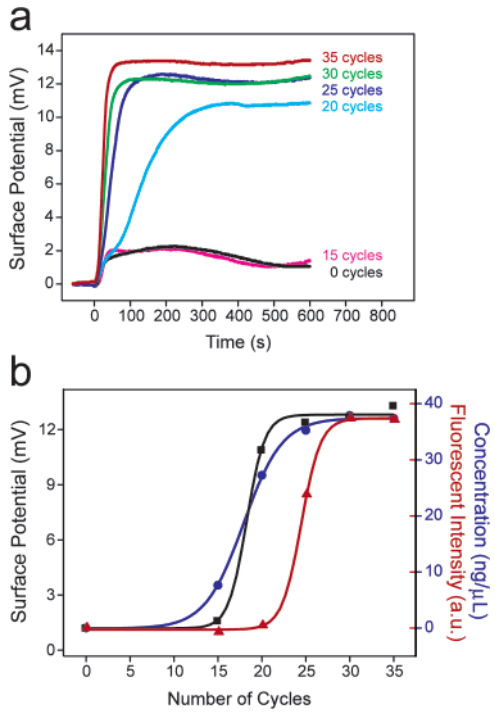

Figure 5. PCR progress monitoring using electronic and optical measurement methods. (a) Real-time electronic surface potential measurements for injections of PCR products. Reaction mixtures terminating after different numbers of cycles (0, 15, 20, 25, 30, 35) were introduced to the electronic sensors for 5 min, followed by 5 min of rinsing. The sensor was regenerated after each measurement by injecting PLL solution. (b) Comparison between steady-state response of electronic measurements (black squares), real-time monitoring of PCR using Sybr Green I intercalating dye at 10 000-fold dilution from stock solution (red triangles), and concentration analysis of the products using DNA Labchip kits (blue circles). No fluorescent labels were used for electronic detection and concentration measurements.

tion. Electronic measurements of PCR experiments terminating after various cycles also showed an increase in output after the 15th cycle, but the steepest rise was registered between the 15th and 20th cycles, as compared to the 20th and 25th cycles for the Sybr Green measurement. To further analyze this discrepancy, the PCR products used for the electronic measurements were also separated and quantified using Labchip kits. As shown in Figure 5b, there is good correspondence between the product concentrations as measured by the Labchip kit and the electronic results. Both sets of data show the largest increase between the 15th and 20th cycles, indicating the electronic readouts were representative of product concentrations. One possible explanation for the discrepancy with the Sybr Green I measurement is that the fluorescent reagent partially inhibits the PCR;[6,7] indeed, we observed total inhibition of PCR reaction when 3 times the manual recommended concentration (10 000× dilution of stock solution) of Sybr Green I dye was included in the PCR mixture at low starting template concentration, which otherwise yielded positive amplification. As a control, we introduced 40 ng/μL of DNA ladder to the electronic sensor before and after analyzing the series of PCR products and observed similar responses. This confirms that the sensitivity of the sensor is preserved throughout the measurements.

For an optical real-time PCR system, the initial template concentration is inversely correlated with the number of cycles required to increase the signal above a threshold level. Since the electronic sensor response increases significantly for DNA concentrations near 10 ng/μL (Figure 3a), this property may be used to define a threshold value similar to that for fluorescent real-time nucleic acid quantification.[4] One could then monitor the number of PCR cycles required for the electronic readout to exceed an experimentally defined threshold value. For example, according to Figure 5b, cycle 15 could be defined as the cycle number needed to create an electronic signal from a starting template concentration of 1 pg/μL. Thus, even though the sensor measures DNA concentrations within a limited range (2.5−80 ng/μL, as shown in Figure 3a), a wider range of starting template concentrations could be measured by determining the number of PCR cycles required to obtain the threshold value.

When compared to approaches based on intercalating dyes, such as Sybr Green I, electronic PCR detection offers similar sensitivity and selectivity but is not prone to inhibition artifacts; however, similar to Sybr Green I, our method detects total amplified products indiscriminately. Thus, it does not offer the additional specificity afforded by hybridization approaches and must, therefore, be viewed as a complement rather than a replacement for sequence-specific, hybridization-based PCR detection schemes. Since the sensor will also detect all dsDNA, to minimize the background signal, one must ensure the starting template concentration is not excessive. In addition, since other negatively charged polyelectrolytes can also potentially bind to the PLL-coated surface,[26] the technique requires samples purified of such species. Moreover, since a portion of the PCR product is consumed during the electronic measurement, to prevent template depletion, the detection volume must be significantly smaller than the PCR reaction volume.

Electronic detection of PCR based on electrostatic association of polyelectrolytes offers several advantages over detection by hybridization. First, there is no need to denature the duplex PCR product as in cases in which immobilized ssDNA is used as capturing probe. Second, the association rate resulting from electrostatic interactions between DNA and PLL is up to 3 orders of magnitude faster than for hybridization events.[29,30] Currently, each measurement requires tens of minutes for each product measurement due to the void volume in our sample delivery system. By incorporating on-chip valves for sample selection,[31] the measurement time could be reduced, and the PLL regeneration of the sensor surface during real-time PCR could be rapidly automated. Third, the structural robustness of layer-by-layer deposition potentially allows multilayers of up to hundreds of layers,[32] and a fresh layer of PLL is deposited before every analytical step. This feature contrasts with techniques that rely on washing to regenerate probe surfaces for additional hybridization experiments. Such regenerations can require harsh conditions and reduce the sensitivity of the sensor by up to 20% between trials due to damage to the functionalized surface.[14]

(30) Yao, D.; Kim, J.; Yu, F.; Nielsen, P. E.; Sinner, E.-K.; Knoll, W. *Biophys. J.* **2005**, *88*, 2745−2751.
(31) Unger, M. A.; Chou, H.-P.; Thorsen, T.; Scherer, A.; Quake, S. R. *Science* **2000**, *288*, 113−116.
(32) Zhang, J.; Senger, B.; Vautier, D.; Picart, C.; Schaaf, P.; Voegel, J. C.; Lavalle, P. *Biomaterials* **2005**, *26*, 3353−61.

One notable feature observed during the surface regeneration step is the characteristic overshoot in surface potential during the injection of the PLL solution. Unlike the binding of DNA, which results in a relatively stable surface potential during rinsing, flushing the sensor with buffer after introducing PLL results in a significant increase in signal and requires additional time to reach equilibrium. In contrast, studies that used surface plasmon resonance spectrometry to monitor the multilayer assembly process did not reveal a sharp change in the signal upon rinsing,[29] suggesting that the polymer did not desorb rapidly due to flushing. It is likely that there is a rearrangement of the polymer or ionic distribution in the film, which in turn changes the potential profile at the film−electrolyte interface.

CONCLUSIONS

Electronic sensing offers a direct, label-free PCR product detection scheme based on the quantification of total amplification product in a PCR mixture. We demonstrated the use of layer-by-layer assembly by specifically detecting amplified DNA in PCR mixtures with a range relevant to the concentrations typically used for PCR. Furthermore, multilayer assembly of DNA and PLL can cover up underlying surface defects and contaminants,[26] making such a system environment-tolerant and potentially feasible for field uses. The system is capable of differentiating nucleic acid concentrations at various stages of PCR by producing a readout that resembles that of fluorescent measurements using intercalating dyes in real-time PCR, but without their potential inhibitory artifacts. By integrating label-free sensing,[8] temperature control capabilities,[33] and on-chip valves for sample manipulation,[31] we envision that the sensing technique will enable a real-time PCR nucleic acid quantification platform without the drawbacks associated with fluorescent optical systems. The electronic sensor substrate can be passivated with silicon oxide, which is known to be compatible with PCR.[8,34] Since PCR protocols can be shortened on a microfabricated silicon device due to its low thermal mass and high thermal conductivity,[35] it might be possible to genotype single cells on an integrated portable device in minutes. Moreover, the ability to electronically monitor PCR amplification on-chip may be a prerequisite for the miniaturization and parallelization of diverse PCR-based technologies ranging from DNA computation to in vitro nucleic acid evolution.

(33) Burns, M. A.; Johnson, B. N.; Brahmasandra S. N.; Handique, K.; Webster, J. R.; Krishnan, M.; Sammarco, T. S.; Man, P. M.; Jones, D.; Heldsinger, D.; Mastrangelo, C. H.; Burke, D. T. *Science* **1998**, *282*, 484−487.

(34) Shoffner, M. A.; Cheng, J.; Hvichia, G. E.; Kricka, L. J.; Wilding, P. *Nuceic Acids Res.* **1996**, *24* (2), 375−379.

(35) Northrup, M. A.; Ching, M. T.; White, R. M.; Watson, R. T. *Transducers '93* **1993**, 924−927.

ACKNOWLEDGMENT

The authors thank Scott Knudsen at University of Texas at Austin and Alex Klibanov, Alice Ting, Tzu-Liang Loh, and Manlin Luo at Massachusetts Institute of Technology for helpful discussions. This work was supported by the Air Force Office of Scientific Research, Hewlett-Packard, and the MIT Sea Grant Program. C.H. acknowledges support from an MIT fellowship and the National Science Foundation Center for Bits and Atoms, and M.G. acknowledges support from the Natural Sciences and Engineering Research Council of Canada (NSERC) through a postdoctoral fellowship. Devices were fabricated in the MIT Microsystems Technology Laboratories.

Received for review November 22, 2005. Accepted January 19, 2006.

AC0520689